doi:10.3969/j.issn.1673-9736.2018.02.07
Article ID: 1673-9736(2018)02-0134-09

Edge detection of potential field data based on image processing methods

TAN Xiaodi, ZHANG Dailei and MA Guoqing

College of Geo-Exploration Science and Technology, Jilin University, Changchun 130026, China

Abstract: The conventional methods of edge detection can roughly delineate edge position of geological bodies, but there are still some problems such as low detection accuracy and being susceptible to noise interference. In this paper, three image processing methods, Canny, LoG and Sobel operators are briefly introduced, and applied to edge detection to determine the edge of geological bodies. Furthermore, model data is built to analyze the edge detection ability of this image processing methods, and compare with conventional methods. Combined with gravity anomaly of Sichuan basin and magnetic anomaly of Zhurihe area, the detection effect of image processing methods is further verified in real data. The results show that image processing methods can be applied to effectively identify the edge of geological bodies. Moreover, when both positive and negative anomalies exist and noise is abundant, fake edge can be avoided and edge division is clearer, and satisfactory results of edge detection are obtained.

Key words: edge detection; image processing; Canny operator; LoG operator; Sobel operator

0 Introduction

Edge detection is very important for the processing and interpreting of potential field data. The edge of anomaly is determined by certain method based on density difference and magnetic difference between geological bodies. In the recent years, plenty of methods have been studied to identify the edge of geological bodies. Horizontal derivative and vertical derivative are widely used in edge enhancement. Nabighian (1972) put forward the analytical signal amplitude (ASM) method, in which maximum value reflects the edge position of objects. Liu *et al.* (2013) used analytical signal and the horizontal derivative to process magnetic data derived from Liangcheng iron ore in Inner Mongolia, and delineated the edge position of ultralow- grade magnetite accurately. Miller and Singh (1994) proposed the tilt angle (Tilt) method, which is the first equalization filter. It can balance anomalies with different amplitude. Ma *et al.* (2012) presented enhanced balancing filter, which can effectively improve the accuracy of edge detection. Wijins *et al.* (2005) put forward the theta map (Theta) method, which also uses maximum value to determine the edge position. Yu *et al.* (2015) utilized normalized differential and theta map to ascertain the locations of the Daxinganling fault zone and the Heihe-Qiqihar-Baicheng fault, which verified the existence of the Heihe-Qigihar-Baicheng fault. The conventional edge detection methods can classify the edge of geological

Received 5 November 2017, accepted 11 December 2017
Supported by projects of the National Key Research and Development Plan (Nos. 2017YFC0602203, 2017YFC0601606), the National Science and Technology Major Project Task (No. 2016ZX05027-002-003), the National Natural Science Foundation of China (Nos. 41604089,41404089), the State Key Program of National Natural Science of China (No. 41430322).

bodies quickly and effectively, but they are still susceptible to noise interference. Furthermore, error information would be produced when positive and negative anomalies exist at the same time. With the continuous development of image processing technology, image edge detection methods have been popularized and applied into many fields. Zhao *et al.* (2008) applied Canny operator into geological mapping of remote sensing. This method can effectively improve the accuracy of edge extraction and divide the boundaries among faults and strata in the study area. Optimized Canny operator (Yang, 2015) was used for the edge detection of gravity and magnetic anomalies, by which the edge points and the noise points were divided effectively, and that the results were ideal. Liu (2016) applied differential operator, LoG operator and Canny operator into the extraction of geological boundary and made a comparison of these methods. The result showed that the color image detection method based on Canny operator can clearly identify the geological boundary and achieve satisfactory effect.

In this paper, three image processing methods are studied and applied to the edge detection of model data and real data. At the same time, three conventional edge detection methods are selected to make a comparison and analysis on the detection effect with image processing methods. These three operators could effectively overcome the defects of conventional methods and get better edge detection results.

1 Methodology

1.1 Canny operator

In image processing, the edge is defined as the position of obvious variations in the grayscale image, and Canny operator is a multilevel edge detection algorithm (Canny, 1986). As the image edge points to different directions, four masks are used to detect image edges in horizontal, vertical and diagonal directions. The same as image processing, Canny algorithm includes four steps for edge detection of potential field data.

(1) Denoising

Noise in original data would seriously interfere edge detection, therefore, the first step is to convolute the original data with 2D Gaussian filter and get a sliding average. Assuming the potential field function is $f(x,y)$, the corresponding Gaussian filter function is

$$G(x,y;\sigma) = \frac{1}{2\pi\sigma^2} e^{-\frac{x^2+y^2}{2\sigma^2}} \tag{1}$$

Where σ is the standard deviation of the Gaussian filter, which controls the smoothness of the filter. The convolution of Gaussian filter and $f(x,y)$ is calculated and the smooth filtering result is obtained

$$\begin{aligned} g(x,y) &= G(x,y;\sigma) * f(x,y) \\ &= \sum_{k=0}^{x-1} \sum_{l=0}^{y-1} g(k,l;\sigma) f(x-k, y-l) \end{aligned} \tag{2}$$

The size of Gaussian filter kernel matrix is determined by the standard deviation (Eshaghzadeh & Salehyan, 2016).

$$\text{size} = 2 \cdot \text{ceil}(2\sigma) + 1 \tag{3}$$

Where the ceil operator takes the smallest integer greater than or equal to the constant in the parenthesis. The size of Gaussian kernel matrix has an important impact on the smoothness of the original data. As it is far less than the size of the data, convolution is carried out in the sliding window. Equation (3) calculates the size of the sliding window. The noise interference is lower with a bigger window, but less details are reflected. On the contrary, the data obtained from the smaller window is susceptible to noise.

(2) Calculating the amplitude and direction of the data gradient

First order finite difference is used to approximately calculate the partial derivatives of the smoothed data in x and y directions. The gradient intensity and direction angle in the data matrix can be obtained respectively by the partial derivatives as

$$\begin{cases} M(x,y) = \sqrt{\left(\dfrac{\partial g(x,y)}{\partial x}\right)^2 + \left(\dfrac{\partial g(x,y)}{\partial y}\right)^2} \\ \theta(x,y) = \arctan\left(\dfrac{\dfrac{\partial g(x,y)}{\partial y}}{\dfrac{\partial g(x,y)}{\partial x}}\right) \end{cases} \tag{4}$$

Where M reflects edge intensity of the data, θ re-

flects the edge direction, and the θ that makes M the local maximum is the edge direction.

(3) Non-maximum suppression

This step is to make the blurred edge of the first step clear. The procedure includes: firstly, the gradient direction of a data point is approximated to one of the angle (0, 45, 90, 135, 180, 225, 270, 315). Then comparing gradient intensity of the point with that of other points in the gradient direction, if the gradient intensity is the maximum, it will be retained, otherwise it is set to zero. Fig. 1 shows a detailed description of the process.

The numbers represent gradient intensity of the data points. The arrow points to the gradient direction. The gradient intensity of four points with gray background in the second row and third row is larger than that of the other points along the gradient direction. Therefore, these numbers will be retained, and the other points will be set to zero.

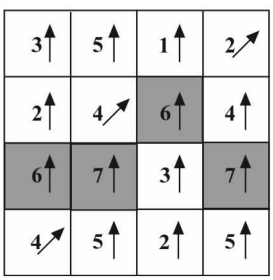

Fig. 1 Explanation of non-maximum suppression

(4) Detection and connection of edge points with dual threshold algorithm

There is still much noise in the data after the non-maximum suppression, and the dual threshold technique in Canny algorithm is used to suppress the noise. After setting upper bound and lower bound of threshold, the data point is regarded as the edge (strong edge) if it is greater than the upper bound. If the point is less than the lower bound, it is not the edge, and it will be considered as an option (weak edge) between the two bounds and needs to be further verified.

In image edge detection, two thresholds, thr_upper and thr_lower are used to process the non-maximum suppression image, and thr_upper = 2.5 × thr_lower. The gray value of the pixels with gradient less than thr_lower pixel is set to zero, and the result is map A. The gray value of the pixels with gradient less than thr_upper is set to zero, and the result is map B. The threshold of map B is higher, in which most of the noise is suppressed and useful edge information would also be lost. The threshold of map A is lower, and more information is retained. Therefore, map A is made as a supplement to connect the image edges based on map B.

Canny algorithm contains many adjustable parameters, which will affect the computing time and the effect of the algorithm.

The size of the Gaussian filter: in the first step, the smooth filter can directly affect the results of Canny algorithm. Smaller filters could produce less blur effect, which can detect smaller and more distinct edges. Larger filters could produce more blur effect, which can detect larger and smooth edges.

Selection of dual threshold: using two thresholds is more flexible than only one, but details would be lost if the threshold is too large, and noise would surpass information of details when the threshold is too small.

Eshaghzadeh and Salehyan (2016) obtained the empirical formula of optimal upper bound threshold after many experiments.

$$T_{upper} = \sqrt{\frac{|S_M - A_M|}{Max_M}} \tag{5}$$

Where S_M, A_M and Max_M represent the standard deviation, average and maximum of the data gradient intensity, respectively. In Canny algorithm, the ratio of the upper bound threshold over the lower bound is generally within [2, 3] (Xiao *et al.*, 2011).

1.2 Laplacian-of-Gaussian operator

Laplacian-of-Gaussian (LoG) operator is an effective edge detection algorithm. First of all, the image is denoised with Gaussian filter and the second derivative is calculated, the edge position of the image is then obtained by detecting zero crossing points of the calculated results (Marr & Hildreth, 1980).

In image edge detection with LoG operator, the Gaussian filter is the same as that of Canny operator. When calculating the partial derivative of the filtered data, the following relationship exists

$$\frac{d}{dt}[G(t;\sigma) * f(t)] = f(t) * \frac{d}{dt}G(t;\sigma) \quad (6)$$

Where $t = (x,y)$. Therefore, the partial derivative of the Gaussian function can be calculated first, and then the convolution would be carried out. According to equation (1), the Gaussian kernel function in convolution can be obtained by simple derivation as

$$\begin{aligned} \mathrm{LoG} &= \left(\frac{\partial^2}{\partial x^2} + \frac{\partial^2}{\partial y^2}\right)G(x,y;\sigma) \\ &= \frac{1}{\sigma^2}\left(\frac{x^2+y^2}{\sigma^2} - 2\right)e^{\frac{-(x^2+y^2)}{2\sigma^2}} \end{aligned} \quad (7)$$

The 2D LoG operator can be approximated by the following 5×5 convolution kernel

$$\begin{bmatrix} 0 & 0 & 1 & 0 & 0 \\ 0 & 1 & 2 & 1 & 0 \\ 1 & 2 & -16 & 2 & 1 \\ 0 & 1 & 2 & 1 & 0 \\ 0 & 0 & 1 & 0 & 0 \end{bmatrix}$$

It is noteworthy that the sum of all elements of the square convolution kernel should be set to zero to ensure that the convolution of the arbitrary homogeneous region is always zero. In the application of edge detection in potential field data, the main steps of the algorithm include:

(1) Implementing LoG convolution with the original data.

(2) Identification of zero crossing points (i. e. transition points from negative to positive or reverse).

(3) Zero crossing points thresholding to suppress weak zero crossing points that may be caused by noise.

1.3 Sobel operator

In the edge detection of image, Sobel operator is also a common method. Sobel operator has two detection directions, one detects the edge of the horizontal direction, and the other detects the edge of the vertical direction. When processing images, Sobel operator weighs the position effect of the pixel points, which can effectively reduce the edge blur to get better effect.

In edge detection of the potential field data, the influence of points in the neighborhood of each data point has different weights. The further the distance is, the smaller the influence is. The weighted sum can be represented by weight function in x and y directions as shown in Fig. 2 (Sobel & Feldman, 1968).

Where the x direction matrix is used as a horizontal operator and signed as W_x. The vertical operator in the y direction is signed as W_y. By convoluting the two operators with the original data respectively, the intensity difference approximation in horizontal and vertical directions can be obtained. Assuming that the original data is D, the data obtained by convolution in horizontal and vertical directions is

$$\begin{cases} S_x = W_x * D \\ S_y = W_y * D \end{cases} \quad (8)$$

The transverse and longitudinal gradient approximation and gradient direction of each data point are respectively

$$\begin{cases} M(x,y) = \sqrt{S_x^2 + S_y^2} \\ \theta(x,y) = \arctan\dfrac{S_x}{S_y} \end{cases} \quad (9)$$

The advantage of Sobel operator is the simple and fast calculation. However, the edge detection effect is not working well for data with complex edge details as only templates along horizontal and vertical directions are used.

1.4 Numerical calculation methods of edge detection

In order to compare the result of edge detection in the potential field data with the three image processing methods mentioned above, three conventional methods of edge detection are introduced, ASM, Tilt and Theta.

ASM calculates the total derivative modulus of the potential field data along three directions (Nabighian, 1972), which is the combination of horizontal and vertical derivatives. Assuming that the data is V

and the expression is

$$ASM = \sqrt{\left(\frac{\partial V}{\partial x}\right)^2 + \left(\frac{\partial V}{\partial y}\right)^2 + \left(\frac{\partial V}{\partial z}\right)^2} \quad (10)$$

The maximum of ASM delineates the edge position of the source, and its main advantage is that the second order derivative of the anomaly is calculated with relatively low noise interference. In addition, the magnetization direction has a low influence on the method for magnetic data. But its shortcoming is also obvious, i. e. the resolution is insufficient.

Tilt is the normalization result of horizontal derivative over vertical derivative (Miller & Singh, 1994), and its expression is

$$Tilt = \arctan\left(\frac{\frac{\partial V}{\partial z}}{\sqrt{\left(\frac{\partial V}{\partial x}\right)^2 + \left(\frac{\partial V}{\partial y}\right)^2}}\right) \quad (11)$$

This method can effectively overcome the problem that the detection effect decreases with the increasing of depth of source. Tilt is usually positive above the source, zero on the edge and negative outside the source, so the edge position can be identified.

Theta (Wijins *et al.*, 2005) obtains the angular cosine between the analytic signal vector and the horizontal plane, and the formula is

$$\cos(\theta) = \frac{\sqrt{\left(\frac{\partial V}{\partial x}\right)^2 + \left(\frac{\partial V}{\partial y}\right)^2}}{\sqrt{\left(\frac{\partial V}{\partial x}\right)^2 + \left(\frac{\partial V}{\partial y}\right)^2 + \left(\frac{\partial V}{\partial z}\right)^2}} \quad (12)$$

The range of cosine value is between [0, 1], and its maximum value corresponds to the source edge. This method can enhance weak anomalies and play a role on balancing anomalies.

The three commonly used edge detection methods have achieved good results in practical applications, but there are still some problems. Therefore, they can be combined with other methods, such as total horizontal derivatives, to achieve better effect. Imaging processing methods are compared with conventional edge detection methods in this paper to verify their effect.

2 Model test

A gravity forward model is built. It contains five prisms with uniform residual density, and there is no overlap among the prisms. The starting coordinates, dimensions and residual density parameters are shown in Table 1, where the unit of length is km, and the unit of density is kg/m^3. Fig. 3 shows the spatial distribution of the prisms. Gravity anomaly of the model is calculated and random noise with power equal to 5% of the peak-to-peak vaule is added. Then the model gravity anomaly is calculated again. The model gravity anomaly and the anomaly with random noise are shown in Fig. 4.

-1	0	1
-2	0	2
-1	0	1

1	2	1
0	0	0
-1	-2	-1

(a) x direction; (b) y direction

Fig. 2 Matrix operators in different directions

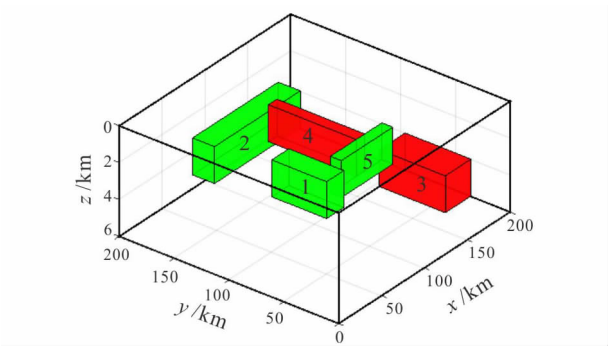

Fig. 3 Spatial distribution of the prisms

The forward model includes positive and negative anomalies, which conforms to the real geological conditions, and the contact area among the prism edges increases the difficulty of edge detection. In addition, adding random noise can reasonably verify the ability of each method on suppressing noise interference. The image processing methods and the numerical edge detection methods are applied to the noisy data, and the

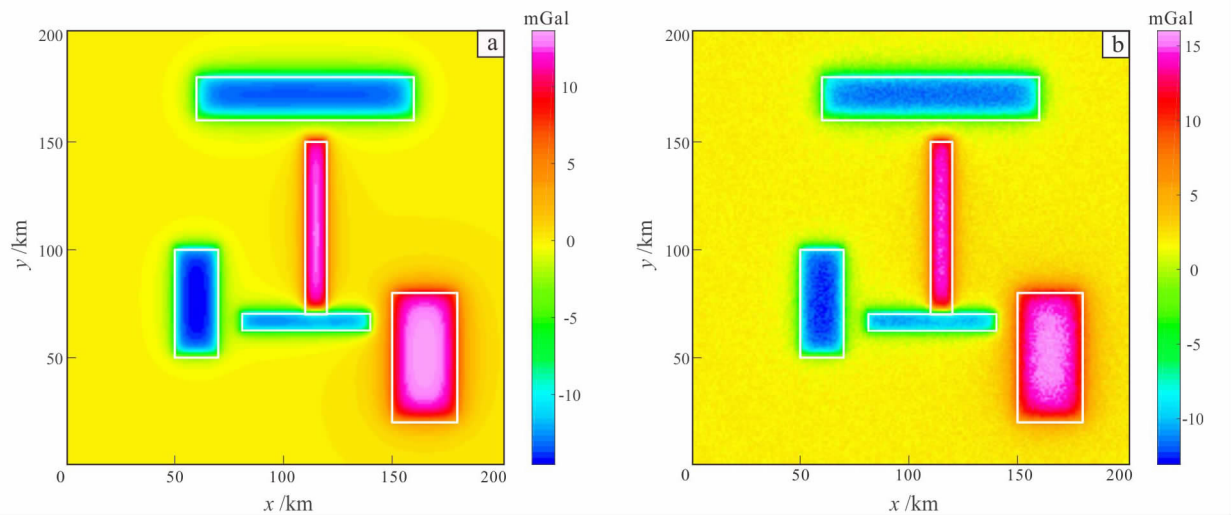

(a) Gravity anomaly without random noise; (b) gravity anomaly contaminated with random noise. The white rectangles denote the horizontal projection position of prisms on the survey plane.

Fig. 4 Gravity anomaly of the model

results are shown in Fig. 5. It can be seen that the three operators can effectively detect the edge of the prisms.

Among them, LoG operator is better in identifying relatively isolated prisms edges, such as the prism 1, 2 and 3. But for the prisms with close contact, fake edge information is introduced. As shown in Fig. 5b, the contact area between prism 4 and 5 has divergent fake edge points, which correspond to the edges of positive and negative anomalies. In addition, there are obvious fake edges at the positive and negative edges of the prisms 2, 4 and 3, 5. It shows that LoG operator is not very effective in identifying the edges between positive and negative anomalies with close distance. However, the overall effect is satisfactory and it is not sensitive to noise. In Fig. 5c, although there is no fake edge in the result of Sobel operator, the edge points of prism 2 and 3 are not focused and it is susceptible to noise. As a more complex algorithm, Canny operator's edge detection results are evaluated to be better. As shown in Fig. 5a, Canny operator dose not introduce fake edges and is less affected by noise, compared with LoG operator and Sobel operator.

The edge detection results of ASM, Tilt and Theta are shown in Fig. 5d-f. It can be seen that all of the methods have basically detected the true edge of the prisms, but they are affected by noise and thus the resolution is insufficient. Especially for ASM, the effect is not ideal in the edge detection of the small prism 4 and 5. Through comparison, it shows that the three operators in this paper achieve better results than conventional methods. Especially for Canny operator, it does not introduce error edge information and is less affected by noise.

Table 1 Position, size and residual density of the prisms

Prism	Starting coordinates	Dimensions	Residual density
1	(50,50,1)	(20,50,2)	-200
2	(60,160,2)	(100,20,2)	-200
3	(150,20,3)	(30,60,2)	200
4	(110,70,1)	(10,80,2)	200
5	(80,60,1)	(60,10,2)	-200

3 Application of real data

In order to verify the edge detection effect of image processing methods in real data application, gravity anomaly data in Sichuan basin and magnetic data in Zhurihe region are used.

First of all, the above methods are used to process gravity data in Sichuan Basin and the results are shown in Fig. 6. Fig. 6a is the Bouguer anomaly, in which the horizontal positions of known faults are marked with white curve (Ma *et al.*, 2012). In Fig. 6c-d, the edge points identified by LoG operator and Sobel operator are more dispersive and do not form continuous edge, which does not match well with known faults. And the results of LoG operator are more scattered in the edge position, which may result in fake edge information due to the noise interference. In Fig. 6b, Canny operator has achieved better results. The detected edge points are continuous and correspond well with the known faults. The trend of faults and more small faults can be identified clearly, and more details are obtained. In Fig. 6e-g, edge detection methods do not get clear edge information. Especially for Tilt and Theta, the resolution is insufficient, and the results are not well matched with known faults.

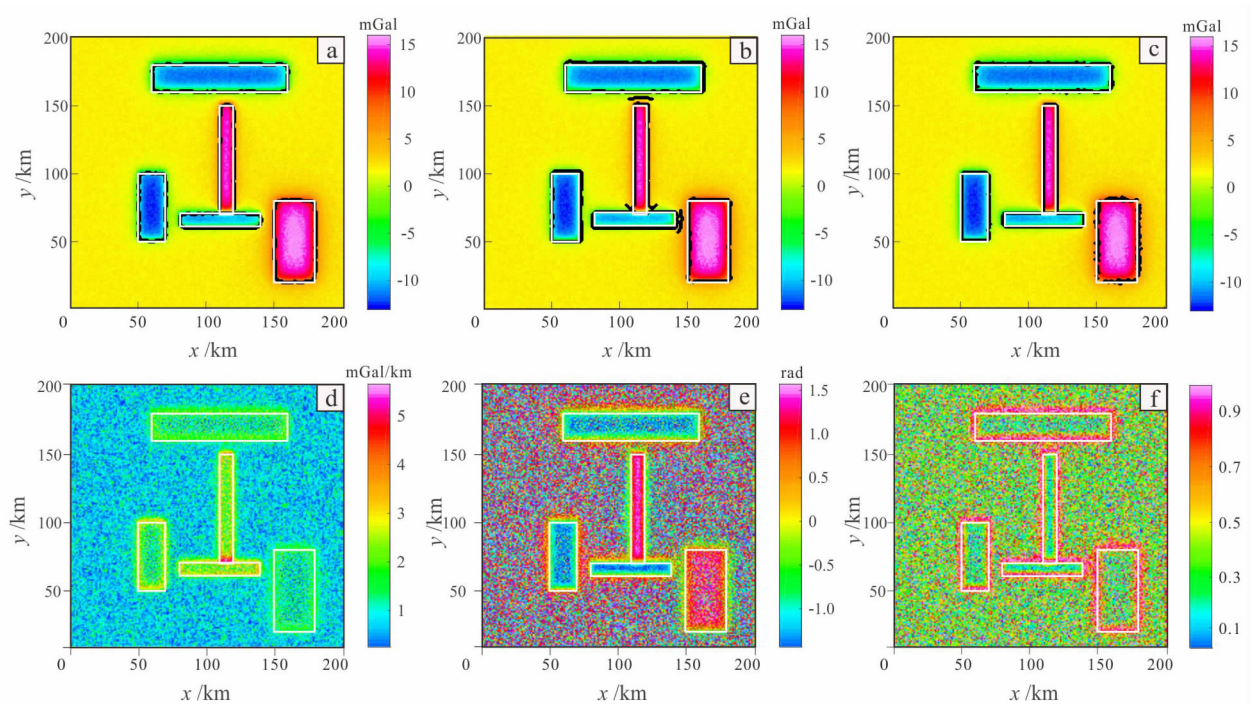

(a) Result of Canny; (b) result of LoG; (c) result of Sobel; (d) result of ASM; (e) result of Tilt; (f) result of Theta. The white rectangles denote the horizontal projection position of prisms on the survey plane, and the black scatters denote edge position detected by the three operators.

Fig. 5 Edge detection results of the model

Magnetic data in Zhurihe region need to be reduced to pole firstly and then the proposed method is used to process the data. As shown in Fig. 7. Fig. 7a is a magnetic anomaly map after being reduced to pole, and it can be seen that the range of the metallogenic belt is clear. According to the application effect of the methods, the resolution of ASM in Fig. 7e is insufficient, which cannot determine accurate edge positions of metallogenic belt. In Fig. 7g, Theta magnifies the noise and introduces fake edge information. In Fig. 7f, Tilt gets better edge detection results, but there are also fake edge points at the upper left corner. From Fig. 7c-d, LoG operator and Sobel operator get better edge position. However, fake information is also introduced and some edge points are scattered. As shown in Fig. 7b, Canny operator clearly delineates the edge of metallogenic belt and corresponds to the known information well.

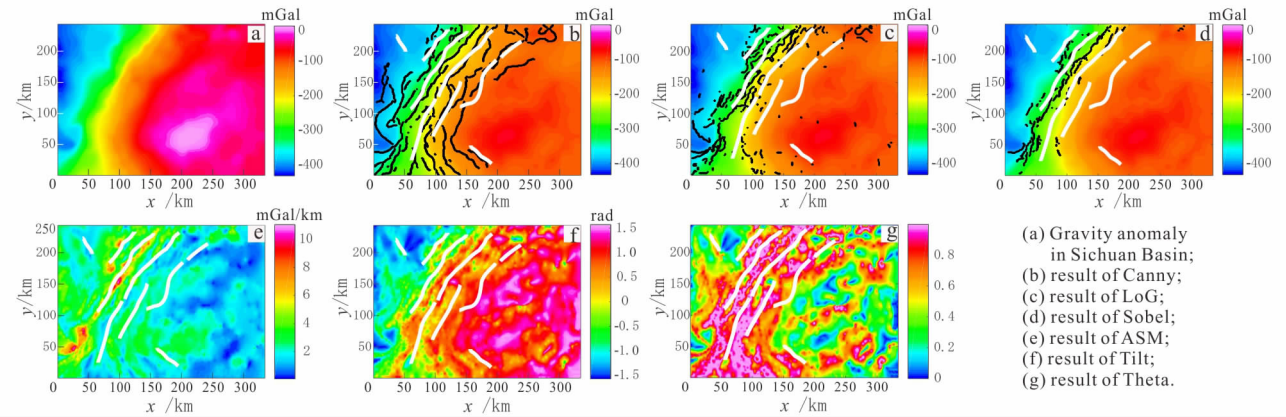

The white lines denote known faults in the field, and black scatters denote edge position detected by the three operators.

Fig. 6 Edge detection results of gravity anomaly of Sichuan Basin

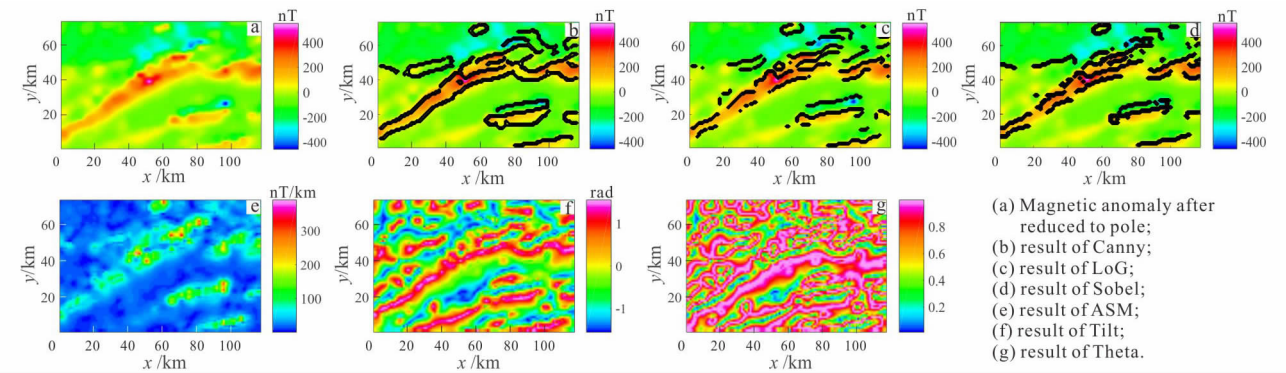

The white lines denote known faults in the field, and black scatters denote edge position detected by the three operators.

Fig. 7 Edge detection results of magnetic anomaly of Zhurihe region

4 Conclusions

(1) The resolution of conventional edge detection methods is usually insufficient. When derivative is further calculated, noise would be magnified, which results in blurry edge position and introduces fake edge information.

(2) The image processing methods discussed in this paper detect edges through calculating horizontal gradient intensity and direction angle of image and determining the extreme points or zero points with threshold. Therefore, the edge detection effect for potential field anomalies with horizontal distribution is better.

(3) Canny operator and LoG operator convolute the original data with 2D Gaussian filter before calculating gradient intensity, which reduces the influence of noise effectively. Sobel operator weighs the position effect of the data points, which can get clearer edge detection results.

References

Canny J F. 1986. A computational approach to edge detection. *IEEE Trans Pattern Analysis and Machine Intelligence*, **8** (6): 679-698.

Eshaghzadeh A, Salehyan N. 2016. Canny edge detection algorithm application for analysis of the potential field map//Iran Conference: 34th National and the 2nd International Geosciences Congress.

Liu G J. 2016. Interface simulation and application research based on geological map: master's degree thesis. Chengdu: Chengdu University of Technology. (in Chinese)

Liu Y B, Zeng Z F, Chen X, *et al*. 2013. Method of analytic

signal and horizontal derivative in magnetic prospecting lean iron deposit: a case study in Liangcheng area, Inner Mongolia. *Global Geology*, **32**(4): 839-846. (in Chinese with English abstract)

Marr D, Hildreth E. 1980. Theory of edge detection. *Proceedings of the Royal Society of London. Series B, Biological Sciences*, **207**: 187-217.

Ma G Q, Huang D N, Yu P, *et al*. 2012. Application of improved balancing filters to edge identification of potential field data. *Chinese Journal of Geophysics*, **55**(12): 4288-4295. (in Chinese with English abstract)

Miller H G, Singh V. 1994. Potential field Tilt-A new concept for location of potential field sources. *Journal of Applied Geophysics*, **32**(2/3): 213-217.

Nabighian M N. 1972. The analytic signal of two-dimensional magnetic bodies with polygonal cross-section: its properties and use for automated anomaly interpretation. *Geophysics*, **37**(3): 507-517.

Sobel I, Feldman G. 1968. A 3x3 isotropic gradient operator for image processing. *Die Pharmazie*, **7**(8).

Wijins C, Perez C, Kowalczyk P. 2005. Theta map: edge detection in magnetic data. *Geophysics*, **70**(4): L39-L43.

Xiao F, Wu Y G, Meng L S. 2011. Edge enhancement and detection technology in gravity anomaly map. *Journal of Jilin University: Earth Science Edition*, **41**(4): 1197-1203. (in Chinese with English abstract)

Yu Q S, Zhang F X, Zeng Z F. 2015. Research on geophysical field in northern part of Da Hinggan mountains. *Global Geology*, **34**(1): 187-193. (in Chinese with English abstract)

Yang S H. 2015. Study on the separation of gravity and magnetic potential field and boundary recognition method: doctor's degree thesis. Chengdu: Chengdu University of Technology. (in Chinese with English abstract)

Yuan Y, Huang D N, Yu Q L. 2015. Using enhanced directional total horizontal derivatives to detect the edges of potential-field full tensor data. *Chinese Journal of Geophysics*, **58**(7): 2556-2565. (in Chinese with English abstract)

Zhao T Y, Zhou K F, Zhang X F, *et al*. 2008. Application of edge detection technology based on Canny algorithms in geological mapping: an example from Baogutu area, the central Asia. *Xinjiang Geology*, (1): 95-99. (in Chinese with English abstract)